Networks and Heterogeneous Media

http://www.aimspress.com/journal/nhm

NHM, 18(3): 946–956.
DOI: 10.3934/nhm.2023041
Received: 27 December 2022
Revised: 12 February 2023
Accepted: 08 March 2023
Published: 20 March 2023

Research article

Mittag-Leffler stability of numerical solutions to linear homogeneous time fractional parabolic equations

Wen Dong[1] **and Dongling Wang**[2,*]

[1] School of Mathematics, Northwest University, Xi'an, Shaanxi, 710127, P.R. China
[2] School of Mathematics and Computational Science, Xiangtan University, Xiangtan, Hunan, 411105, P.R. China

* **Correspondence:** Email: wdymath@xtu.edu.cn, wdyxtu@126.com.

Abstract: In a bounded domain, the solution of linear homogeneous time fractional parabolic equation is known to exhibit polynomial type decay rate (the so-called Mittag-Leffler stability) over time, which is quite different from the exponential decay of classical parabolic equation. We firstly use the finite element method or finite difference method to discretize the parabolic equation in space to obtain fractional ordinary differential equation, and then use fractional linear multistep method (F-LMM) to discretize in time to obtain a fully discretized schemes. We prove that the strongly A-stable F-LMM method combined with appropriate spatial discretization can accurately maintain the long-term optimal algebraic decay rate of the original continuous equation. Numerical examples are included to confirm the correctness of our theoretical analysis.

Keywords: sub-diffusion equation; Mittag-Leffler stability; polynomial decay rate; fractional LMM

1. Introduction

Let $\Omega \subset \mathbb{R}^d$ be a bounded domain with smooth boundary $\partial\Omega$. Consider the initial-boundary value problem for a time-fractional parabolic equation:

$$D_t^\alpha u(x,t) - \mathcal{L}u(x,t) = 0, \quad x \in \Omega, \quad t \geq 0, \tag{1.1}$$

subject to the Dirichlet-boundary condition $u(x,t) = 0$ for $x \in \partial\Omega$ and the initial value $u(x,0) = u_0(x), x \in \Omega$. Here $D_t^\alpha u(t) := \frac{1}{\Gamma(1-\alpha)} \int_0^t (t-s)^{-\alpha} u'(s)ds$ denote the Caputo time fractional derivative of order $\alpha \in (0,1)$ and $\mathcal{L}$ be a linear second-order elliptic operator in $H^2(\Omega) \cap H_0^1(\Omega)$

$$(\mathcal{L}u)(x,t) = \sum_{i,j=1}^d \partial_i(a_{ij}(x)\partial_j u(x)) + \sum_{j=1}^d b_j(x)\partial_j u(x) + c(x)u(x,t). \tag{1.2}$$

Like [1], we assume that $a_{ij} = a_{ji} > 0$ in $\overline{\Omega}$, and also either $c \geq 0$ or $c - \frac{1}{2}\sum_{j=1}^{d} \partial_j b_j \geq 0$ to ensure the existence and uniqueness of the solution.

The time fractional parabolic equation with order $\alpha \in (0, 1)$ include diffusion, sub-diffusion equation and other types, which are often used to describe various transport processes with memory effect. The existence, uniqueness and stability of solutions of fractional partial differential equations (F-PDEs) have been deeply studied and many important results have been obtained. Many typical results, such as fractional comparison principle [2] and maximum principle [3], have been established. Compared with the standard parabolic equation, the solution of the anomalous parabolic model (1.4) has two typical characteristics [4]:

- weak singularity at $t = 0$. That is the solution of the equation pointwise satisfies the estimation $\left|\frac{\partial^k u(x,t)}{\partial t^k}\right| \leq C(1 + t^{\alpha-k})$. In particularly, for $k = 1$ we have

$$|u'(\cdot, t)| \leq C\left(1 + t^{\alpha-1}\right)\|u_0\|_{L^2(\Omega)},\ \textit{i.e.},\ \|u'(\cdot, t)\|_{L^2(\Omega)} \to +\infty \text{ as } t \to 0^+; \tag{1.3}$$

- long-time polynomial decay rate,

$$\|u(\cdot, t)\|_{L^2(\Omega)} \leq \frac{C}{1 + t^{\alpha}}\|u_0\|_{L^2(\Omega)} = O(t^{-\alpha}) \text{ as } t \to +\infty. \tag{1.4}$$

In this paper, we mainly focus on the long time behavior of numerical solution. In [5], it is pointed out that the asymptotic stability and long-time decay behavior of solution to linear homogeneous Caputo time fractional ordinary differential equations (F-ODEs) are completely determined by the eigenvalues of the coefficient matrix. For the F-PDE, the optimal long time estimation of the solution is also established [6–8]. Similarly, asymptotic stability also applies to fractional systems obtained from different practical problems. Examples include fractional-order coupled reaction-diffusion neural networks without strong connectedness [9], fractional-order memristor neural networks with leakage delay [10], time fractional reaction-diffusion systems with unknown time-varying input uncertainties [11], and non-autonomous fractional order neural networks with impulses [12]. The asymptotic stability of exact discretization numerical scheme for Caputo-Hadamard fractional differential equation on the time scale is proved in [13].

In [5], the authors proves that the numerical solutions of the linear homogeneous F-ODEs are Mittag-Leffler stable by singularity analysis of the generating function, which shows the numerical solution completely preserves the same optimal decay rate for a long time as that for the continuous equation. In this paper, we first convert the F-PDE into a F-ODE system through the finite element method or finite difference method in the spatial direction, and then use the methods and ideas from [5] to prove that for a large class of strongly A-stable numerical methods, the numerical solution can accurately maintain the long-time decay rate of the continuous equation.

The main work of this paper is to establish the numerical Mittag-Leffler stability of F-PDEs and obtain the same long-time decay rate of the numerical solution as that of the continuous solution. The detailed description can be expanded from the following aspects:

- For homogenous F-PDEs, we use two spatial discretization methods to obtain time F-ODEs, and then use strong A-stable fractional linear multistep methods (F-LMMs) to get the corresponding generating function equation of numerical solution.

- We mainly use the singularity analysis of the generating function to establish the Mittag-Leffler stability conditions of numerical solution for the fully discretized scheme.

The rest of the paper is organized as follows. In Section 2, we first review the properties of solution for F-ODE system. Then we derive the space semi-discretization scheme by finite element or finite difference for Eq (1.4) and combine with F-LMMs to obtain the fully discretized schemes. In Section 3, we prove the numerical solution preserves the long-time decay rate $O(t_n^{-\alpha})$. Numerical examples are included in Section 4.

2. Numerical methods for F-PDE

Let us start with the main results on Mittag-Leffler stability for F-ODE system.

Lemma 2.1. [14] *Consider the F-ODE system $D_t^\alpha y(t) = Ay(t)$ where $y \in \mathbb{R}^d$ and A is a constant coefficient matrix. Let λ_A be the eigenvalue of matrix A. Then it holds that*

(i) The solution to F-ODE is asymptotically stable if and only if all the eigenvalues λ_A satisfy that

$$\lambda_A \in \Lambda_\alpha := \{z \in \mathbb{C}\backslash\{0\} : |\arg(z)| > \frac{\alpha\pi}{2}\}. \tag{2.1}$$

(ii) If all the eigenvalues $\lambda_A \in \Lambda_\alpha$, the solution to the F-ODE is Mittag-Leffler stable, i.e., $\|y(t)\| = O(t^{-\alpha})$ as $t \to \infty$.

2.1. Spatial discretization methods

In order to apply the main results and ideas of F-ODE, we first discretize the equation in space. We will consider two typical methods, namely the finite element method and the finite difference method.

2.1.1. Finite difference approximation

Let $\bar{\Omega}_h$ be the tensor product of $d = 2$ uniform meshes $\{ih\}_{i=0}^M$, where $\Omega_h := \bar{\Omega}_h\backslash\partial\Omega$ denotes the set of interior mesh nodes. Now, consider the spatial difference semidiscretization

$$\begin{cases} D_t^\alpha u(x,t) = \mathcal{L}_h u(x,t), \quad x \in \Omega_h, \quad t > 0, \\ u(\cdot,t) = 0 \;\; in \;\; \bar{\Omega}_h \cap \partial\Omega, \quad u(x,0) = u_0 \;\; in \;\; \bar{\Omega}_h, \end{cases} \tag{2.2}$$

where $\mathcal{L}_h$ is a standard central differential operator defined by

$$\begin{aligned} \mathcal{L}_h u(x,t) := \sum_{p,q=1}^{2} \frac{1}{2} h^{-2} \{ & a_{pq}(x+h\delta_p)[u(x+h\delta_p,t) - u(x+h\delta_p-h\delta_q,t)] \\ & + a_{pq}(x-h\delta_p)[u(x-h\delta_p,t) - u(x-h\delta_p+h\delta_q,t)] \\ & + a_{pq}(x)[u(x+h\delta_q,t) - 2u(x,t) + u(x-h\delta_q,t)]\} \\ & - \sum_{p=1}^{2} \frac{1}{2} h^{-1} b_p(x)[u(x+h\delta_p,t) - u(x-h\delta_p,t)] - c(x)u(x,t). \end{aligned} \tag{2.3}$$

Then the spatial finite difference semi-discrete scheme of Eq (1.4) can be written as

$$D_t^\alpha u^h = L_h u^h, \tag{2.4}$$

where L_h is the spatial difference matrix.

The local truncation error of the solution of the above semi-discrete scheme is known to be $O(h^2)$ under the condition $h^{-1} \geq \max_{k=1,2}\left\{\frac{1}{2}\|b_k\|_{L_\infty(\Omega)}\|a_k^{-1}\|_{L_\infty(\Omega)}\right\}$ in the norm $L_\infty(\Omega)$ [15]. In the following finite element semi-discrete scheme, when the coefficient satisfies $c - \frac{1}{2}\sum_{k=1}^{2}\partial_k b_k \geq 0$, it can also be obtained that the local truncation error is $O(h^2)$.

2.1.2. Finite element method

Let $V_h \subset H_0^1(\Omega) \cap C(\bar{\Omega})$ be the Lagrange finite element space of a quasi-uniform simplical triangulation $\mathcal{T}$ of Ω. Let $u^h \in V_h$ satisfy

$$\langle D_t^\alpha u^h, v^h\rangle_h = \mathcal{A}_h(u^h, v^h), \quad \forall v^h \in V_h \tag{2.5}$$

with $u_0^h = u_0$, and $\langle\cdot,\cdot\rangle_h$ is an approximation of the inner product $L_2(\Omega)$. Let $\langle\cdot,\cdot\rangle$ denoting the exact $L_2(\Omega)$ inner product, then the bilinear from $\mathcal{A}_h$ is defined by $\mathcal{A}_h(u, v) := \langle\mathcal{L}u - cu, v\rangle + \langle cu, v\rangle_h$ [15]. We construct an approximation of the solution in a family of finitely dimension subspaces:

$$V_h := \left\{\rho^i\right\}_{i=1}^{M+1}, \quad (\rho^i, \rho^j) = \delta_{ij},$$

where $\{\rho^i\}_{i=1}^{M+1}$ is an orthonormal basis of V_h. So we have $u^h = \sum_{i=1}^{M+1}(u^h, \rho^i)\rho^i$, and when we take $v^h = \rho^j$, Eq (2.5) can be rewritten as

$$D_t^\alpha \sum_{i=1}^{M+1}(u^h, \rho^i)\left\langle\rho^i, \rho^j\right\rangle_h = \sum_{i=1}^{M+1}(u^h, \rho^i)\mathcal{A}_h(\rho^i, \rho^j). \tag{2.6}$$

This leads to the finite element semi-discrete scheme for Eq (1.4)

$$D_t^\alpha u^h = L_h u^h \tag{2.7}$$

with $L_h \in \mathbb{R}^{(M+1)\times(M+1)}$ determined by $L_1^{-1}L_2$, where $L_1(i, j) = \langle\rho^i, \rho^j\rangle_h$ and $L_2(i, j) = \mathcal{A}_h(\rho^i, \rho^j)$. Since L_1 is known as the identity matrix, there is $L_h := L_2$. Therefore, for the two spatial discretization methods, we have a unified form as that given in Eqs (2.4) and (2.7), but L_h has a different meanings.

2.2. Time discretization method and generating function

We recall some basic concepts and notations. Let $\delta_d := (1, 0, 0, \ldots)$ be the convolution identity and $\delta_{i,j}$ be the Kronecker function. Denote $u = (u_0, u_1, \ldots)$, where $u_n \in \mathbb{C}^1$, be a discrete sequence. When $u,\ v$ are two scalar sequences, we define the discrete convolution $v * u = \omega$, where $\omega_n = \sum_{j=0}^{n} v_{n-j}u_j$. The sequence v is said to be invertible only if $v * u = \delta_d$ and u is the inverse of v, i.e. $u = v^{-1}$. The generating function for $u = (u_0, u_1, \ldots)$ is defined as $F_u(z) = \sum_{n=0}^{\infty} u_n z^n,\ \ z \in \mathbb{C}$. Then it is easy to to see if $v * u$, then $F_{v*u}(z) = F_v(z)F_u(z)$ and if $\omega = \mu^{-1}$ then $F_\mu(z) = 1/F_\omega(z)$.

In Eq (1.4), let u_n be the approximation of $u(\cdot, t_n)$ by implicit scheme on uniform grid $t_n = n\tau$ with step size $\tau > 0$ in the form

$$D_\tau^\alpha(u_n) := \frac{1}{\tau^\alpha}\sum_{j=0}^{n}\mu_j(u_{n-j} - u_0) = L_h u_n, \quad n \geq 1. \tag{2.8}$$

In order to include $n = 0$, Eq (2.8) can be rewritten as

$$\frac{1}{\tau^\alpha}\sum_{j=0}^{n}\mu_j(u_{n-j} - u_0) = L_h(u_n - u_0\delta_{n,0}), \quad n \geq 0.$$

Let $\omega = \mu^{-1}$. By generating function we have $u - u_0 = \tau^\alpha \omega * L_h(u_n - u_0\delta_{n,0})$, then

$$u_n - u_0 = \tau^\alpha[\omega * L_h(u_n - u_0\delta_{n,0})]_n = \tau^\alpha\left(\sum_{j=0}^{n}\omega_{n-j}L_h u_j - \omega_n L_h u_0\right), \quad n \geq 0. \tag{2.9}$$

In Eqs (2.8) and (2.9), the coefficients $\{\mu_n\}$ and $\{\omega_n\}$ can be determined in several ways. Perhaps the most famous method is the convolution quadrature (CQ) developed by Lubich [16, 17], which inherits the excellent numerical stability characteristics of the classical linear multistep method (LMM). Another important method is the L1 scheme [4]. Here we list the generating functions of several widely used methods; see Table 1 or [5].

Table 1. Numerical methods and their generating functions.

Methods	$F_\omega(z)$	$F_\omega(0)$
F-BDF1	$(1-z)^{-\alpha}$	1
F-BDF2	$(1-z)^{-\alpha}(\frac{3-z}{2})^{-\alpha}$	$(\frac{3}{2})^\alpha$
F-Adams2	$(1-z)^{-\alpha}(1-\frac{\alpha}{2}(1-z))$	$1-\frac{\alpha}{2}$
L1 scheme	$\frac{z}{(1-z)^2}Li_{\alpha-1}^{-1}(z)$	1

By generating function $F_\omega(z) = \sum_{j=0}^{\infty}\omega_j z^j$, as long as $F_\omega(z)$ is given, the corresponding coefficients $\{\mu_n\}$ and $\{\omega_n\}$ will be determined accordingly. In summary, we obtain the fully discretized scheme for Eq (1.4):

$$u_n = u_0 + \tau^\alpha\sum_{j=1}^{n}\omega_{n-j}L_h u_j, \quad n \geq 1. \tag{2.10}$$

3. Numerical Mittag-Leffler stability for F-PDEs

We now analyze the long-term qualitative behavior of the numerical solution of the fully discretized scheme (2.10) for F-PDEs. We first review some related concepts and results of numerical solution for F-ODEs [5, 17].

3.1. Numerical stability region of F-LMMs

The linear test model for F-ODEs (with $\alpha \in (0, 1)$) is $D_t^\alpha y(t) = \lambda y$, which is asymptotic stable if $\lambda \in \Lambda_\alpha$, as indicated in Lemma 2.1. Applying F-LMMs to the fractional linear test equation gives

$$y_n = y_0 + \lambda\tau^\alpha[\omega * (y - y_0\delta_d)]_n, \quad n \geq 0. \tag{3.1}$$

The numerical stability region for Eq (3.1) is defined by

$$\mathcal{S}_\tau^\alpha := \{\zeta = \lambda\tau^\alpha \in \mathbb{C}\setminus\{0\} : y_n \to 0 \text{ as } n \to \infty\}, \tag{3.2}$$

and a numerical method is said to be $A(\beta)$-stable (with $\beta \in (0,\pi)$), if the region $\mathcal{S}_\tau^\alpha$ contains the infinite wedge $A(\beta) = \{z \in \mathbb{C} \setminus \{0\}; |\arg(-z)| < \beta\}$. Similarly to ordinary differential equations (ODEs), if the stability region $\mathcal{S}_\tau^\alpha$ contains the entire sector Λ_α, i.e., $\mathcal{S}_\tau^\alpha \supset \Lambda_\alpha$, then the method is said to be $A(\frac{\alpha\pi}{2})$-stable, or simply A-stable.

Consider the classical k-step LMMs with generating polynomials $\rho(z) = \sum_{j=0}^k \alpha_j z^j$ and $\sigma(z) = \sum_{j=0}^k \beta_j z^j$. Let

$$\delta(z) = \frac{z^k \rho(z^{-1})}{z^k \sigma(z^{-1})} = \frac{\alpha_0 z^k + \cdots + \alpha_{k-1} z + \alpha_k}{\beta_0 z^k + \cdots + \beta_{k-1} z + \beta_k}.$$

The LMM defined by a generating polynomial $F_{\overline{\omega}}(z) = F_{\overline{\omega}(\rho,\sigma)}(z) = \delta(z)^{-1}$ for the classical ODE, with order $p \geq 1$ is called strong $A(\beta)$-stable if

$$\begin{aligned} &\delta(z) \text{ is analytic, with no zeros in a neighborhood of the unit disk } |z| \leq 1 \text{ except } z = 1; \\ &|\arg \delta(z)| \leq \pi - \beta \text{ for } |z| < 1; \ \ \tfrac{1}{\tau}\delta\left(\mathrm{e}^{-\tau}\right) = 1 + O\left(\tau^p\right), \text{ with } p \geq 1\,. \end{aligned} \tag{3.3}$$

See [16,17]. The fundamental relationship between the stability regions of the classical LMMs and the F-LMMs is given by

Lemma 3.1. [17] *Consider a classical LMM defined by a generating polynomial* $F_{\overline{\omega}}(z) = \delta(z)^{-1}$ *satisfies the stability conditions Eq* (3.3). *Let* $\mathcal{S}_\tau$ *and* $\mathcal{S}_\tau^\alpha$ *be the stability regions of the standard LMM and its corresponding F-LMM defined by* $F_\omega(z) = (F_{\overline{\omega}}(z))^\alpha = \delta(z)^{-\alpha}$ *respectively. Then it holds that*

(i) $\mathcal{S}_\tau^\alpha = \mathbb{C} \setminus \{1/F_\omega(z) : |z| \leq 1\}$;

(ii) $(\mathbb{C} \setminus \mathcal{S}_\tau^\alpha) = (\mathbb{C} \setminus \mathcal{S}_\tau)^\alpha$;

(iii) *LMM is A-stable if and only if the F-LMM is A-stable;*

(iv) *with* $\pi - \varphi = \alpha(\pi - \psi)$, *LMM is* $A(\varphi)$*-stable if and only if the F-LMM is* $A(\psi)$*-stable.*

The above stability results are extended to general finite dimensional F-ODE systems in [5].

Lemma 3.2. [5, Theorem 7] *Assume that the F-LMM satisfies the conditions in* (3.3). *Then for the vector-valued F-ODEs* $D_t^\alpha u(t) = Au$ *with any step size* $\tau > 0$, *the numerical stability region is given by*

$$\begin{aligned} \mathbb{S}_\tau^\alpha &= \det\left(I - \tau^\alpha F_\omega(z) A\right) \neq 0 \ for\ |z| \leq 1 \\ &\Leftrightarrow \frac{1}{\tau^\alpha F_\omega(z)} \ \textit{is not an eigenvalue of matrix A for}\ |z| \leq 1 \\ &\Leftrightarrow \mathbb{C} \backslash \left\{ \frac{1}{\tau^\alpha F_\omega(z)} \ \textit{is an eigenvalue of matrix A for}\ |z| \leq 1 \right\}. \end{aligned}$$

Lemma 3.2 shows that if $\lambda_A \in \Lambda_\alpha$ and the F-LMMs are strongly A-stable, then $\det\left(I - \tau^\alpha F_\omega(z) A\right) \neq 0$ for all $|z| \leq 1$ and $\tau > 0$. This leads to the F-LMMs is unconditionally stable for the vector-valued F-ODEs.

3.2. Mittag-Leffler stability analysis

Generating function is the main tool to study the long time behavior of numerical solutions for time fractional differential equations. The following lemma gives the internal relationship between the coefficient of generating function and the behavior of function singularity at $z = 1$.

Lemma 3.3. [18] *Assume $F_u(z)$ is analytic on $\Delta(R,\theta) := \{z : |z| < R,\ z \neq 1,\ |\arg(z-1)| > \theta\}$ for some $R > 1$ and $\theta \in (0, \frac{\pi}{2})$. If $F_u(z) \sim (1-z)^{-\beta}$ as $z \to 1$, $z \in \Delta(R,\theta)$ for $\beta \neq \{0,-1,-2,-3,\cdots\}$, then $u_n \sim \frac{1}{\Gamma(\beta)} n^{\beta-1}$ as $n \to \infty$.*

In the following, we study the polynomial long time decay rate for the numerical solution of Eq (1.4). So before we do that we first need to check that L_h satisfies the condition of Lemma 3.3.

When h is so small such that $h^{-1} \geq \max_{k=1,2}\left\{\frac{1}{2}\|b_k\|_{L_\infty(\Omega)}\|a_k^{-1}\|_{L_\infty(\Omega)}\right\}$, then the spatial central difference operator $\mathcal{L}_h$ satisfies the discrete maximum principle. Hence, $-L_h$ is an M-matrix. It is also known from [1, Remark 7.2] that the matrix associated with the spatial linear finite element discretized operator $-\mathcal{A}_h$ is also an M-matrix. So the real part of the eigenvalue of the semi-discrete matrix L_h is less than 0, i.e. $\lambda_{L_h} \in \mathbb{C}^-$. The strong stability condition for F-LMMs yields $1/F_\omega(z)$ falls in region $\{z : |\arg z| \leq \frac{\alpha\pi}{2}\} \cap \mathbb{C}^+$. Therefore $1/(\tau^\alpha F_\omega(z))$ is not an eigenvalue of L_h, which leads to that

$$\det(I - \tau^\alpha F_\omega(z)L_h) \neq 0, \text{ for all } |z| \leq 1 \text{ and } \tau > 0. \tag{3.4}$$

Theorem 1. *Assume the F-LMMs is strong A-stable in the fully discrete scheme* (2.10) *for F-PDE* (1.4)*. Then the numerical solution is Mittag-Leffler stable, i.e., $\|u_n^h\| = O(t_n^{-\alpha})$ as $n \to \infty$ for any $\tau \geq 0$.*

Proof. It follows from Eq (2.10) that $u_n^h = u_0^h + \tau^\alpha \sum_{j=1}^n \omega_{n-j} L_h u_j^h$, then

$$u_n^h = (I - \tau^\alpha \omega_n L_h)u_0^h + \tau^\alpha \sum_{j=0}^n \omega_{n-j} L_h u_j^h.$$

Multiply the above equation both sides by z^n and sum over n form 0 to ∞ to get that

$$F_{u^h}(z) = \sum_{n=0}^\infty (I - \tau^\alpha \omega_n L_h) z^n u_0^h + \tau^\alpha F_\omega(z) L_h F_{u^h}(z). \tag{3.5}$$

From Eq (3.5), we can get

$$\begin{aligned}
F_{u^h}(z) &= (I - \tau^\alpha F_\omega(z)L_h)^{-1}\left(\frac{1}{1-z}I - \tau^\alpha F_\omega(z)L_h\right)u_0^h \\
&= (I - \tau^\alpha F_\omega(z)L_h)^{-1}\left(I - \tau^\alpha F_\omega(z)L_h + \frac{z}{1-z}I\right)u_0^h \\
&= \left(I + \frac{z}{1-z}(I - \tau^\alpha F_\omega(z)L_h)^{-1}\right)u_0^h.
\end{aligned}$$

We see from Eq (3.4) that the inverse $(I - \tau^\alpha F_\omega(z)L_h)^{-1}$ exists for $|z| \leq 1$ and $z \neq 1$. And the generating polynomial constructed under the condition of strong A-stability satisfies that [5], $F_\omega(z) \sim (1-z)^{-\alpha}$ as $z \to 1$. So we have

$$\begin{aligned}
F_{u^h}(z) &= \left[I + \frac{z}{1-z}(I - \tau^\alpha(1-z)^{-\alpha}L_h)^{-1}\right]u_0^h \\
&= \left[I + \frac{z}{(1-z)^{1-\alpha}}\frac{1}{\tau^\alpha}\left(\frac{(1-z)^\alpha}{\tau^\alpha}I - L_h\right)^{-1}\right]u_0^h \\
&= \frac{1}{(1-z)^{1-\alpha}}\left[(1-z)^{1-\alpha}I + \frac{z}{\tau^\alpha}\left(\frac{(1-z)^\alpha}{\tau^\alpha}I - L_h\right)^{-1}\right]u_0^h.
\end{aligned}$$

Since $0 < \alpha < 1$, we have $(1-z)^{1-\alpha} \to 0$ and $(1-z)^{\alpha} \to 0$ as $z \to 1$. Therefore, we have $F_{u^h}(z) \sim \frac{1}{(1-z)^{1-\alpha}} \cdot \frac{1}{\tau^{\alpha}} L_h^{-1} u_0^h$ as $z \to 1$. By Lemma 3.3, we have $u_n^h \sim \frac{1}{\Gamma(1-\alpha)} L_h^{-1} u_0^h n^{-\alpha} \tau^{-\alpha}$, which lead to the desired results $\|u_n^h\| \sim O(t_n^{-\alpha})$ as $n \to \infty$. □

4. Numerical example

To quantitatively investigate the long-time decay rate of the numerical solution, we introduce the index function

$$p_\alpha(t_n) = -\frac{\ln(\|u_{n+5}^h\|/\|u_n^h\|)}{\ln(t_{n+5}/t_n)}, \tag{4.1}$$

which is numerical observation order of decay rate as $O(t_n^{-p_\alpha})$. It is independent of the initial value. In the numerical example we take $\Omega = [0,1]^2$, the initial value $u_0 = 10\sin(4\pi x)\sin(4\pi y)$ and the parameter $a_{11} = a_{22} = 2,\ a_{12} = a_{21} = 1,\ b_1 = b_2 = 1,\ c = 1$.

Table 2. Observed p_α computed by $L1$ scheme in time and finite difference and finite element (the values in brackets) in space with $\tau = 0.2,\ h = \frac{1}{32}$.

t_n	$\alpha = 0.1$	$\alpha = 0.3$	$\alpha = 0.5$	$\alpha = 0.7$	$\alpha = 0.9$
100	0.1003(0.1003)	0.3013(0.3013)	0.5026(0.5026)	0.7038(0.7038)	0.9049(0.9049)
300	0.1000(0.1000)	0.3004(0.3004)	0.5008(0.5008)	0.7013(0.7013)	0.9016(0.9016)
500	0.0999(0.0999)	0.3002(0.3002)	0.5005(0.5005)	0.7008(0.7008)	0.9010(0.9010)
700	0.0999(0.0999)	0.3001(0.3001)	0.5004(0.5004)	0.7006(0.7006)	0.9007(0.9007)
900	0.0999(0.0999)	0.3001(0.3001)	0.5003(0.5003)	0.7004(0.7004)	0.9005(0.9005)

Table 3. Observed p_α computed by BDF1 scheme in time and finite difference and finite element (the values in brackets) in space with $\tau = 0.2,\ h = \frac{1}{32}$.

t_n	$\alpha = 0.1$	$\alpha = 0.3$	$\alpha = 0.5$	$\alpha = 0.7$	$\alpha = 0.9$
100	0.1004(0.1004)	0.3018(0.3018)	0.5039(0.5039)	0.7064(0.7064)	0.9052(0.9052)
300	0.1000(0.1000)	0.3005(0.3005)	0.5013(0.5013)	0.7020(0.7020)	0.9030(0.9030)
500	0.1000(0.1000)	0.3003(0.3003)	0.5008(0.5008)	0.7013(0.7013)	0.9018(0.9018)
700	0.0999(0.0999)	0.3002(0.3002)	0.5005(0.5005)	0.7009(0.7009)	0.9013(0.9013)
900	0.0999(0.0999)	0.3001(0.3001)	0.5004(0.5004)	0.7007(0.7007)	0.9010(0.9010)

We calculate and observe index p_α with various choices of parameters for F-BDF1 and $L1$ schemes, as shown in Table 2 and Table 3 respectively, from which the decay rate data is completely consistent with our theoretical prediction of Theorem 1, i.e., $O(t_n^{-\alpha})$.

Figure 1 shows the numerical solutions of U^n at the initial time $t_n = 0$, and Figures 2, 3, 4 are the numerical solutions U^n at the time $t_n = 10, 30, 100$, respectively. From Figure 1 to Figure 4, it can be

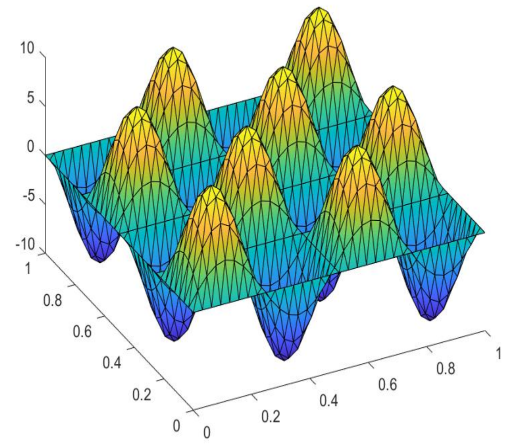

Figure 1. U_0.

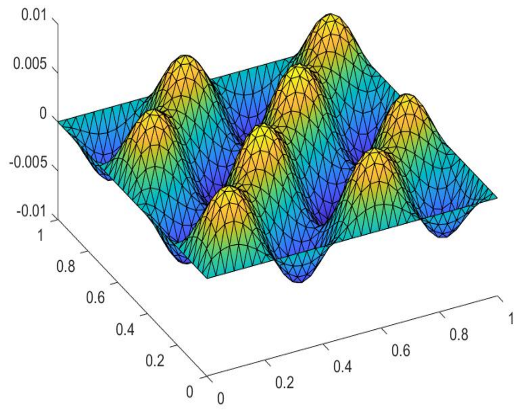

Figure 2. U^n for $t_n = 10$.

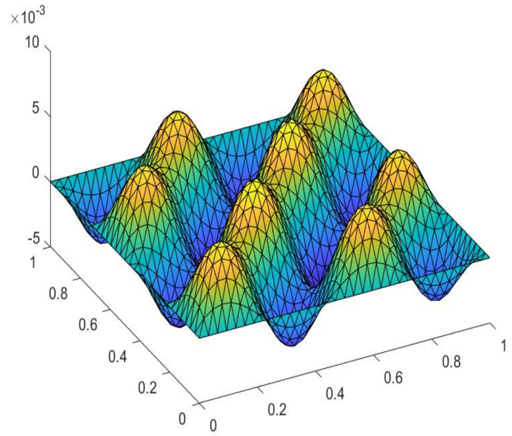

Figure 3. U^n for $t_n = 30$.

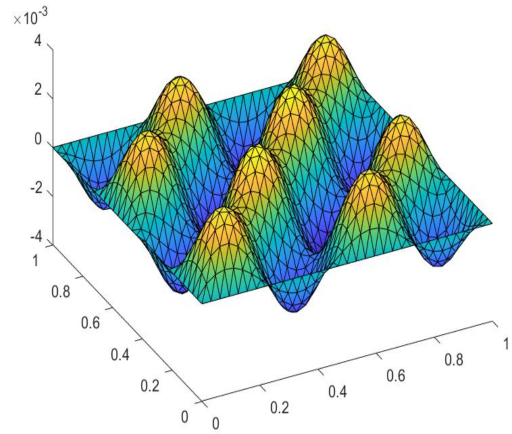

Figure 4. U^n for $t_n = 100$.

seen that the $\|U^n\|$ of the numerical solution decays with time, and further qualitative analysis can get that $\|U^n\| = O(t_n^{-\alpha})$, as expected.

Acknowledgments

The second author is partially supported by NSFC grant 12271463 and Fund of Hunan Provincial Education Department 22B0173.

Conflict of interest

The authors declare there is no conflict of interest.

References

1. N. Kopteva, Error analysis for time-fractional semilinear parabolic equations using upper and lower solutions, *SIAM J. Numer. Anal.*, **58** (2020), 2212–2234. https://doi.org/10.1137/20M1313015
2. B. Jin, *Fractional Differential Equations*, Cham: Springer, 2021.
3. Y. Luchko, Initial-boundary-value problems for the one-dimensional time-fractional diffusion equation, *Fract. Calc. Appl. Anal.*, **15** (2012), 141–160. https://doi.org/10.2478/s13540-012-0010-7
4. M. Stynes, A survey of the L1 scheme in the discretisation of time-fractional problems, *Numer. Math. Theory Methods Appl.*, **15** (2022), 1173–1192. https://doi.org/10.4208/nmtma.OA-2022-0009s
5. D. L. Wang, J. Zou, Mittag-Leffler stability of numerical solutions to time fractional ODEs, *Numer. Algorithms*, **3** (2022). https://doi.org/10.1007/s11075-022-01379-8
6. K. Adam, R. Katarzyna, Y. Masahiro, *Time-Fractional Differential Equations: A Theoretical Introduction*, Singapore: Springer, 2020, 109–119. https://doi.org/10.1007/978-981-15-9066-5
7. M. D'Abbicco, G. Girardi, Asymptotic profile for a two-terms time fractional diffusion problem, *Fract. Calc. Appl. Anal.*, **25** (2022), 1199–1228. https://doi.org/10.1007/s13540-022-00041-3
8. R. Zacher, Time fractional diffusion equations: solution concepts, regularity, and long-time behavior, in *Volume 2 Fractional Differential Equations*, Berlin/Munich/Boston: Walter de Gruyter GmbH, 2019, 159–180. https://doi.org/10.1515/9783110571660-008
9. Y. Cao, Y. G. Kao, J. H. Park, H. B. Bao, Global Mittag-Leffler stability of the delayed fractional-coupled reaction-diffusion system on networks without strong connectedness, *IEEE Trans. Neural Netw. Learn. Syst.*, **33** (2022), 6473–6483. https://doi.org/10.1109/TNNLS.2021.3080830
10. Y. G. Kao, Y. Li, J. H. Park, X. Y. Chen, Mittag–Leffler synchronization of delayed fractional memristor neural networks via adaptive control, *IEEE Trans. Neural Netw. Learn. Syst.*, **32** (2021), 2279–2284. https://doi.org/10.1109/TNNLS.2020.2995718
11. F. D. Ge, Y. Q. Chen, Event-triggered boundary feedback control for networked reaction-subdiffusion processes with input uncertainties, *Inf. Sci.*, **476** (2019), 239–255. https://doi.org/10.1016/j.ins.2018.10.023
12. Y. G. Kao, H. Li , Asymptotic multistability and local S-asymptotic ω-periodicity for the nonautonomous fractional-order neural networks with impulses, *Sci. China Inf. Sci.*, **64** (2021), 112207. https://doi.org/10.1007/s11432-019-2821-x
13. G. C. Wu, T. T. Song, S. Q. Wang, Caputo-Hadamard fractional differential equations on time scales: Numerical scheme, asymptotic stability, and chaos, *Chaos*, **32** (2022), 093143. https://doi.org/10.1063/5.0098375
14. D. Matignon, Stability results for fractional differential equations with applications to control processing, *Comput. Eng. Syst. Appl. Multiconf.*, **2** (1996), 963–968.
15. N. Kopteva, Error analysis of the L1 method on graded and uniform meshes for a fractional-derivative problem in two and three dimensions, *Math. Comp.*, **88** (2017), 2135–2155. https://doi.org/10.1090/mcom/3410

16. C. Lubich, Discretized fractional calculus, *SIAM J. Math. Anal*, **17** (1986), 704–719. https://doi.org/ 10.1137/0517050

17. C. Lubich, Fractional linear multistep methods for Abel-volterra integral equations of the second kind, *Math. Comp.*, **45** (1985), 463–469. https://doi.org/10.1090/S0025-5718-1985-0804935-7

18. P. Flajolet, R. Sedgewick, *Analytic Combinatorics*, Cambridge: Cambridge University Press, 2009.